Journal of Mammalian Evolution, Vol. 12, Nos. 3/4, December 2005 (© 2005)
DOI: 10.1007/s10914-005-6958-x

New Study on Dental and Skeletal Features of the Cretaceous "Symmetrodontan" Mammal *Zhangheotherium*

Zhe-Xi Luo[1,3] and Qiang Ji[2]

A new partial skeleton of the Cretaceous "symmetrodontan" mammal *Zhangheotherium quinquecuspedens* from the Yixian Formation of Liaoning, China has shed light on the dental and skeletal features of this taxon. The new fossil is a juvenile individual of late growth stage, preserved with interesting features of the premolar replacement. This fossil also provides new information on the vertebral column, the pelvis, the hindlimb and pes. *Zhangheotherium* has a typical diphyodont replacement of its premolars that is characterized by an alternating pattern (p1 → p3 → p2). This alternating replacement of premolars is a derived condition shared by *Dryolestes*, *Slaughteria*, and some basal eutherians, and differs from the plesiomorphic sequential replacement of anterior postcanines in eutricondontans, in most multituberculates and in stem mammaliaforms. The calcaneus and astragalus in the ankle joint of *Zhangheotherium* lack superposition. This shows that the trechnotherian clade, of which *Zhangheotherium* is a basal taxon, has retained the primitive condition of mammaliaforms in which the astragalus is in juxtaposition with the calcaneus. Coupled with recent evidence from the earliest metatherians and eutherians, this suggests that the superposition of astragalus and calcaneus evolved in parallel in metatherians and eutherians.

KEY WORDS: *Zhangheotherium*, Trechnotherians, premolar replacement pattern, ankle morphology.

INTRODUCTION

The Early Cretaceous witnessed the first appearance of eutherian and metatherian mammals on the northern Laurasian continents and the rise of the toothed monotremes in Australia and their proximal relatives on southern Gondwanan continents (Kielan-Jaworowska *et al*., 2004). An important source of new information on early mammalian evolution during the Early Cretaceous is in the Lagerstätte of the Yixian Formation of Liaoning, China, which in recent years yielded an unprecedented number of relatively complete mammalian skeletons. The diverse mammals discovered so far from the Yixian Formation include the earliest-known eutherian (*Eomaia*, Ji *et al*., 2002), the earliest-known metatherian (*Sinodelphys*, Luo *et al*., 2003), two "symmetrodontans" or stem trechnotherians (*Zhangheotherium*, Hu *et al*., 1997, 1998; *Maotherium*, Rougier *et al*., 2003), several eutriconodontans (*Jeholodens*, Ji

[1] Section of Vertebrate Paleontology, Carnegie Museum of Natural History, Pittsburgh, Pennysylvania 15213, USA.
[2] Institute of Geology, The Chinese Academy of Geological Sciences, Beijing 100037, China.
[3] To whom correspondence should be addressed at Section of Vertebrate Paleontology, Carnegie Museum of Natural History, Pittsburgh, Pennysylvania 15213, USA. E-mail: LuoZ@CarnegieMNH.Org

et al., 1999; *Repenomamus*, Li *et al*., 2001; Wang *et al*., 2001; Hu *et al*., 2005; *Gobiconodon*, Li *et al*., 2003), and at least one multituberculate (*Sinobaatar*, Hu and Wang, 2002).

Zhangheotherium and *Maotherium* are the proximal relatives to spalacotheriid "symmetrodontan" mammals from the Jurassic and Cretaceous of Europe and North America (Simpson, 1928; Fox, 1976, 1985; Prothero, 1981; Hu *et al*., 1998; Sigogneau-Russell and Ensom, 1998; Cifelli and Madsen, 1999; Gill, 2004). Although *Zhangheotherium* and *Maotherium* are distinctive from all currently known spalacotheriids in certain plesiomorphic dental characteristics, these two taxa share a long list of derived characters with spalacotheriids characterized by acute-angled molars. These two "symmetrodontan" mammals from the Yixian Formation are closely related to each other, and have been included in the family Zhangheotheriidae (Rougier *et al*., 2003). They are stem taxa within the trechnotherian clade defined by the common ancestor of *Zhangheotherium*, extant placentals and marsupials (*sensu* McKenna, 1975), plus all other extinct relatives that are nested within this clade by current phylogenetic estimates (Prothero, 1981; Luo *et al*., 2002).

The new fossil material of *Zhangheotherium* is from the Sihetun site in the Yixian Formation in western Liaoning Province. The site has been dated at 125 million years (Swisher *et al*., 1999; although see Lo *et al*., 1999). The fossil is preserved on a light gray shale slab with eosesthyrid conchostracans and some plant debris (Fig. 1). No counter-part of this slab fossil is available.

SYSTEMATICS

Mammalia
Trechnotheria (McKenna, 1975)
Zhangheotheriidae (Rougier *et al*., 2003)
Zhangheotherium (Hu *et al*., 1997)
Z. quinquecuspedens (Hu *et al*., 1997)

Taxonomic Affinities

The new specimen (CAGS-IG99-07352: Chinese Academy of Geological Sciences, Institute of Geology, Beijing, China; Fig. 1) resembles most closely the holotype specimen of *Z. quinquecuspedens* (IVPP V7466, Institute of Vertebrate Paleontology and Paleoanthropology, Beijing, China). It differs from the holotype specimen of *Maotherium sinensis* (NGMC 97415) in several dental characters. *Maotherium* is distinguished from *Zhangheotherium* primarily by the upper molar characters (Rougier *et al*., 2003). Moreover, the lower molars of *Maotherium* have more reduced posterior cusp c and taller cusp b; so that cusps b and c are asymmetrical relative to primary cusp a. By contrast, cusps b and c on lower molars in *Zhangheotherium* are nearly of the same height and are symmetrical with respect to cusp a. Both *Z. quinquecuspedens* and *M. sinensis* show a gradient of decreasing size of the more posterior lower molars but this tendency is far more pronounced in *Maotherium* holotype than in *Zhangheotherium* holotype. *Maotherium* is a smaller taxon than *Zhangheotherium*, with smaller size of skeletal elements and teeth. However, its dentition shows a more mature (older) dental development age according to the stage of eruption of the more posterior molars (Rougier *et al*., 2003).

The new specimen (CAGS97-07352) under our study shows equal size of the lower cusps b and c, more similar to *Z. quinquecuspedens* than to *M. sinensis*. Its teeth are more

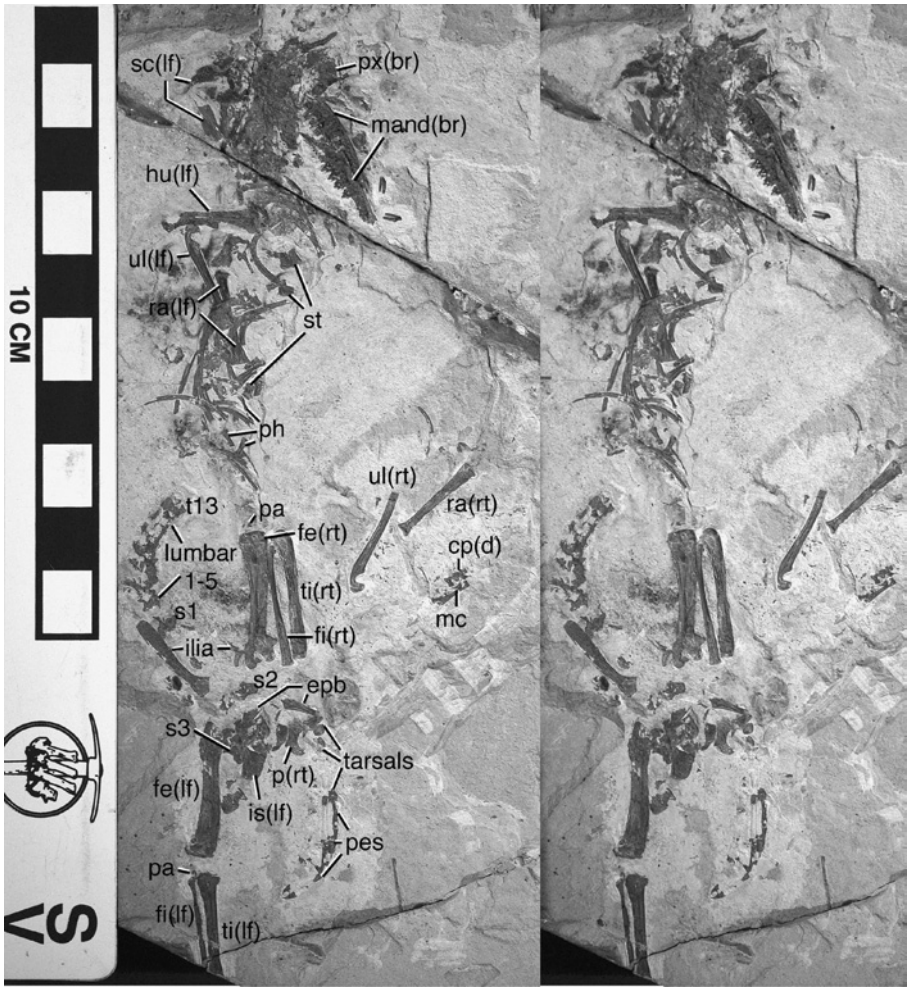

Fig. 1. Stereo photos of an incomplete specimen of *Z. quinquecuspedens* (Chinese Academy of Geological Sciences: CAGS97-07352; a juvenile individual). Abbreviations: cp(d), (distal) carpals; epb, epipubes (left and right); fe, femur; fi, fibula; hu(lf), humerus-left; is(lf), ischium-left (exposed in dorsomedial view); mand(br), mandibles (broken); mc, metacarpals; p(rt), pubis-right (exposed in lateral view); pa, patella (partially ossified, in both the left and right); ph, phalanges; px(br), broken premaxilla; ra, radius; s1, s2, s3, sacral vertebrae 1–3; sc(lf), scapula-left (broken); st, scattered sternal elements; ti, tibia; t13, ul, ulna.

comparable in size to those of *Zhangheotherium*, slightly larger than those of *Maotherium*, but show a much earlier stage of dental replacement than the holotype of *M. sinensis* (Fig. 2; Table I). The prevalent evidence available so far suggests that CAGS97-07352 is a juvenile individual of *Z. quinquecuspedens*. Our new observation on CAGS97-07352 and our review of the distinctive dental characteristics of *Z. quinquecuspedens* and *M. sinensis* corroborate the argument that *Maotherium* is a distinctive taxon from *Zhangheotherium* (Rougier *et al*., 2003).

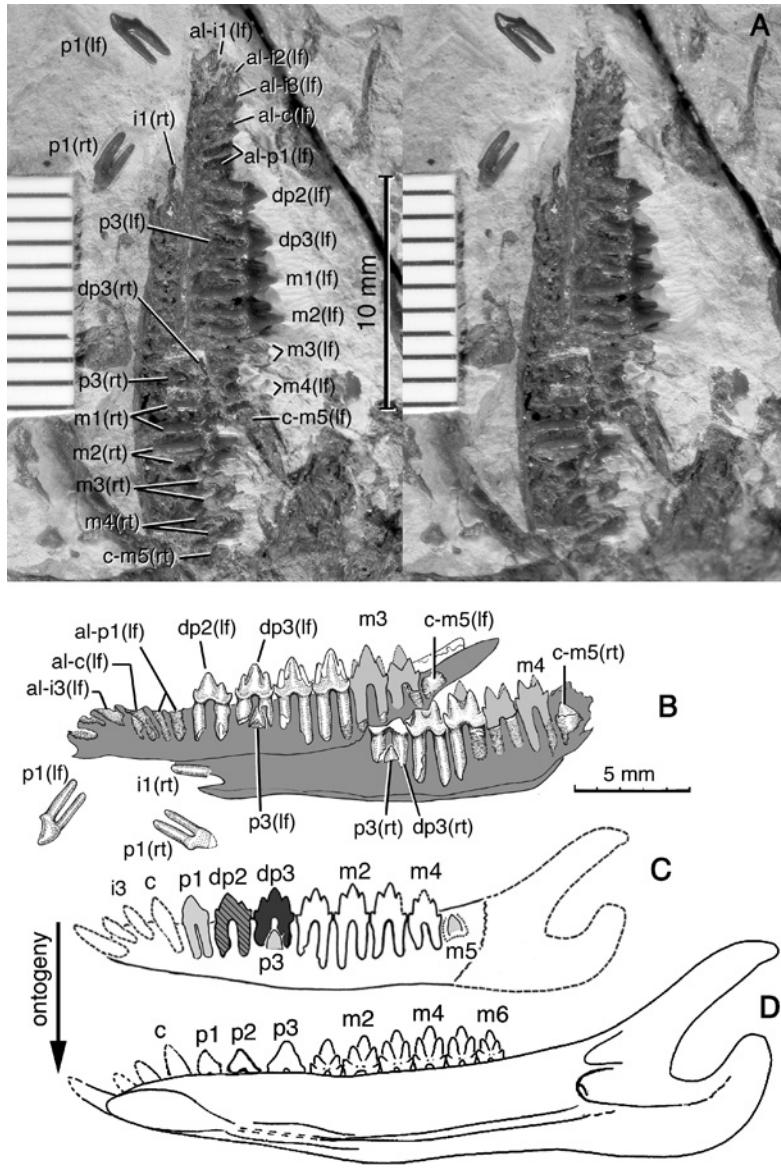

Fig. 2. Dental features of *Zhangheotherium* juvenile (CAGS97-07352) and pattern of dental replacement. (A) Stereo photos of damaged left and right mandibles with full exposure to the roots and erupting teeth in the juvenile specimen of *Zhangheotherium*. (B) Interpretive illustration of the mandibles, dentition, and dental replacement features (light gray—outline of molars represented by mold-impression and damaged crown; dark gray—the interior of mandible exposed in the damaged fossil). (C) Inferred dental replacement from juvenile (CAGS97-07352) (light gray—incipient or newly erupted teeth; hatched pattern and dark gray—deciduous teeth). (D) subadult (IVPP 7466; modified after Hu *et al*., 1998) in a growth series of *Zhangheotherium*. Abbreviations: al-alveolus; c-m5(lf), empty crypt for the lost m5 in left mandible; c-m5(rt), m5 developing within crypt in right mandible; i, c, p, m, incisor, canine, premolar, molar; (lf), left side; (rt), right side.

Our determination that CAGS97-07352 represents a late-stage juvenile individual of *Zhangheotherium* is based on the fact that two deciduous premolars are retained at the posterior premolar loci and the ultimate molar (m5) has partially formed within the dental crypt but not yet erupted. CAGS97-07352 has only four fully functional molars by comparison to the five functional molars in the holotype of *Z. quinquecuspedens*. Moreover, CAGS97-07352 is smaller than the holotype of *Z. quinquecuspedens* (IVPP 7466); long bones in its forelimb and hindlimb are only about 75 to 85% for the homologous long bones in the forelimb and hindlimb in the holotype of *Z. quinquecuspedens* (Table I). Given the difference in size and in dental replacement stage, we consider CAGS97-07352 and the holotype of *Z. quinquecuspedens* to be a late stage juvenile and a subadult, respectively. Both the new juvenile specimen (CAGS97-07352) and the subadult-type specimen of *Z. quinquecuspedens* (IVPP 7466) have unfused epiphyseal growth plates between the diaphysis (shaft) and epiphyses of the long bones. By contrast, in the majority of extant placentals, the epiphyseal growth plates are fused in mature adults.

The incomplete skull is compressed and most of the bones are not recognizable (Fig. 1). Damage to the mandibles has exposed features relevant to the assessment of dental replacement. Otherwise this specimen offers little new information on the cranial anatomy

Table I. Measurement and Comparison of Skeletal Elements and Teeth[a]

	Zhangheotherium		*Maotherium*
	IVPP 7466[b] Length (mm)	CAGS97-07352 Length in (mm)	NGMC97415[c] *Maotherium*
Bone			
Humerus	22.1	17.1 (left)	
Ulna	21.5	18 (right)	17.6
		17.5 (left)	
Radius	17.1	15.4 (left)	15.1
		15.2 (right)	
Metacarpal III	6.5	5.8 (left)	6.0
Ilium	20.1	15.8 (left)	16.3–16.8
Ischium	8.5	7.5 (right)	8.5–8.6
Pubis	—		
Epipubis	9.1	7.7 (left)	6.5+
Femur	22	22 (left)	23
Tibia	23.5	21 (left)	22
Fibula	23.5	19.5 (left)	20.3
Calcaneus	6.6	6.1 (left)	
Metatarsal III	8.6	7.9 (left)	7.3
p2 or dp2		1.6 (dp2)	1.4–1.5
p3 or dp3		1.7 (dp3)	1.6–1.7
m1	1.5	1.6	1.5–1.5
m2	1.6	1.7	1.5–1.5
m3	1.8	1.6	1.4–1.4
m4	1.7	1.45	1.3–1.3
m5	1.5		1.1–1.1
m6	1.1		0.5–0.6

[a] Measurements and comparisons are for the new (CAGS97-07352) and holotype (IVPP 7466) of *Z. quinquecuspedens* and *M. sinensis* (NGMC97415).
[b] Based on Hu *et al.* (1997).
[c] Based on Rougier *et al.* (2003).

of *Zhangheotherium*. Our new anatomical observation will focus on the dentition and the postcranial features that were not available from other specimens of zhangheotheriids.

DENTITION

The lower dentition of *Zhangheotherium* comprises: i3, c1, p3, m5, herein revised from the previous dental count (Hu *et al*., 1997, 1998) on the basis of new materials. In the new fossil of CAGS97-07352, bone of the mandibles is macerated (Fig. 2) and all dental alveoli, roots of functional teeth, partially formed tooth crown and the crypt for developing permanent teeth are fully exposed in both mandibles. The three lower incisors of the left mandible are represented by three alveoli, which correspond precisely to the three single-rooted incisors in the holotype of *Zhangheotherium*. The first lower incisor (i1) is fully procumbent, as preserved in the right mandible (Fig. 2) and this incisor has a large alveolus in the left mandible. Two other incisors, i2 and i3, are smaller and less procumbent, as shown by their respective alveoli. The lower canine is single-rooted.

The first lower permanent premolar is two-rooted, with long and straight roots typical of the permanent teeth. Its crown has an asymmetrical cusp a, plus a small posterior cingulid cuspule. There is no trace of any deciduous premolar (dp1) at the p1 locus. The labial side of p1 is slightly more convex than the lingual side (Fig. 2). Deciduous p2 is in position and has not been shed. The deciduous nature of this tooth is indicated by the irregular shape and the very short length of its roots, plus a nearly "molariform" crown. In all these features, dp2 here is similar to the deciduous premolars of the "eupantothere" *Dryolestes* (Martin, 1997, 1999). The crown of dp2 crown is characterized by main cusp a, small anterior cusp b near the cingulid level, conspicuous posterior cusp c, and distal cingulid cuspule d. The triangulation of the cusps is not strongly developed in dp2. Dp3 is fully molariform with cusps b and c symmetrical with respect to main cusp a. Mesial cingulid cusp e and distal cingulid cusp d are present. The deciduous nature of dp3 is evidenced by the irregular shape and shortness of its roots, and the permanent p3 has partially formed between the roots of the deciduous tooth. In the permanent p3, only the primary cusp a (protoconid) is fully calcified but the rest of the crown is not yet developed.

Given that replacing p3 is already partially formed and at least one root of dp3 is already absorbed, prior to the formation of the replacing p2 under the intact roots of dp2 in either the left or the right mandible, it is certain that the replacement at the p3 locus will occur prior to the replacement at the p2 locus. Because the permanent p1 is already in position, it is most likely the replacement at the p1 locus has already occurred. In summary, the chronological sequence of premolar replacement in *Zhangheotherium* is: p1 $\rightarrow$ p3 $\rightarrow$ p2 (Fig. 2).

The juvenile specimen (CAGS97-07352) and subadult (IVPP 7466) of *Z. quinquecuspedens*, if arranged in a growth series according to their "dental age" and their size, can help demonstrate that this mammal has one generation of replacement of lower premolars, in an alternate pattern and in an antero-posterior sequence (Fig. 2) (Luo *et al*., 2001). Among the three lower premolars, permanent p1 erupted first, followed then by shedding of dp3 and eruption of permanent p3, and lastly by replacement at the p2 locus. The replacement at the p3 locus occurs around the time of eruption of m5, as expected from the fact that permanent p3 and m5 have about the same degree of development in crypts. The replacement at the p2 locus occurs around the time of eruption of m6, which has not yet developed in the juvenile

CAGS97-07352 but is present in the subadult IVPP 7466. Thus the sequence of replacement is: p1 → p3 → p2, both for the shedding of deciduous teeth and for eruption of permanent teeth. In all premolar loci, the deciduous predecessor tooth is more "molariform" than its permanent successor.

Premolar replacement has been documented in spalacotheriids of North America, which are closely related to *Zhangheotherium*. In North American Cretaceous spalacotheriids, the deciduous premolars are known to be associated with these spalacotheriid taxa from the same fossil sites (Cifelli, 1999). However, the North American spalacotheriids are not complete enough to show if the premolar replacement was either alternating or sequential. Extrapolating from the close relationships of spalacotheriids and *Zhangheotherium*, it is conceivable that spalacotheriids may have similar alternate premolar replacement as in *Zhangheotherium*. There is no evidence that molars are replaced in *Zhangheotherium*, nor in any spalacotheriids. The comparative significance of this pattern will be discussed in the next paragraphs.

The first three molars (m1–3) are almost identical in morphology. The primary cusp a (protoconid) is the tallest cusp of the crown; anterior cusp b (paraconid) and posterior cusp c (metaconid) are of equal height and symmetrical with respect to cusp a. Similar to *Zhangheotherium* holotype and *Maotherium*, the major cusps (a, b, c) are conical and cusps b and c are well separated from cusp a. The crests between cusps a and b and cusps a and c are not as well developed in *Zhangheotherium* and *Maotherium* as in spalacotheriids (Prothero, 1981; Fox, 1985; Sigogneau-Russell and Ensom, 1998; Cifelli and Madsen, 1999). These plesiomorphies (more conical cusps and less-developed shearing crests) are the primary basis for separating zhangheotheriids from the typical spalacotheriids (Hu *et al*., 1998; Cifelli and Madsen, 1999; Rougier *et al*., 2003). There are a small mesial cingulid cuspule e and a small distal cingulid cuspule d. The mesial cingulid cuspule e of the succeeding molar is lingual to the distal cuspule d of a preceding molar, so that cuspule d and cuspule e of the succeeding tooth overlap each other by an imbricating interlock. All lower molars lack crest-like, distinctive cingulids on both the labial and lingual sides, although the crown shows gibbousness and slightly overhangs the root at the crown-root junction. Unlike the irregular roots of dp2 and dp3, m1 through m4 have very straight roots that are proportionately longer. The ultimate m5 is still in its crypt in the left mandible, and only primary cusp a on its crown is fully calcified. In the posterior part of the right mandible, a crypt for the developing m5 is present, although the tooth crown of m5 is lost, presumably due to the damage of the specimen.

Major wear facets are under-developed or absent in the newly erupted molars but become increasingly better developed in molars that had been functional for longer duration, after removing a certain amount of enamel at the contact surface. This is a pattern seen in *Maotherium* (Rougier *et al*., 2003) and with wide systematic distribution in mammaliaforms (Mills, 1984; Crompton and Luo, 1993). In the more worn molars, a large wear facet is present on the anterolabial face of the tooth between cusp b and a; and this is equivalent to wear facet 1 (following Crompton, 1971). Another large wear facet is present on the posterolabial face of the crown between cusp c and a, which is equivalent to wear facet 2.

A noteworthy plesiomorphy of the new specimen of *Zhangheotherium* is the gradient of molar cusp triangulation. The angle formed by cusps a, b and c is more obtuse in anterior molars and more acute in posterior molars. Similar gradation of molar cusp triangulation along the molar series is developed to various extents in kuehneotheriids, amphiodontids,

and spalacotheriids (Crompton and Jenkins, 1967; Cifelli and Madsen, 1999; Averianov, 2002; Luo *et al*., 2002), and in gobiconodontids (Kielan-Jaworowska and Dashzeveg, 1998).

SKELETON

Forelimb

The right humerus is partially preserved, and the outline of the bone in the matrix shows that the posterior aspect of the distal humeral articulation to the ulna is trochlea-like, confirming an earlier observation that the ulnar condyle is vestigial (Hu *et al*., 1998). Other preserved forelimb elements include the complete radius, ulna, the four distal carpals, and some scattered and incomplete carpals and phalanges. These elements of CAGS97-07352 add little to what is already known from the better-preserved holotype specimen of *Zhangheotherium* (IVPP 7466).

Axial Skeleton

Four sternal elements can be recognized (Fig. 3). The interclavicle is identified by a similar shape of this element to the interclavicle in the holotype of *Zhangheotherium*. The

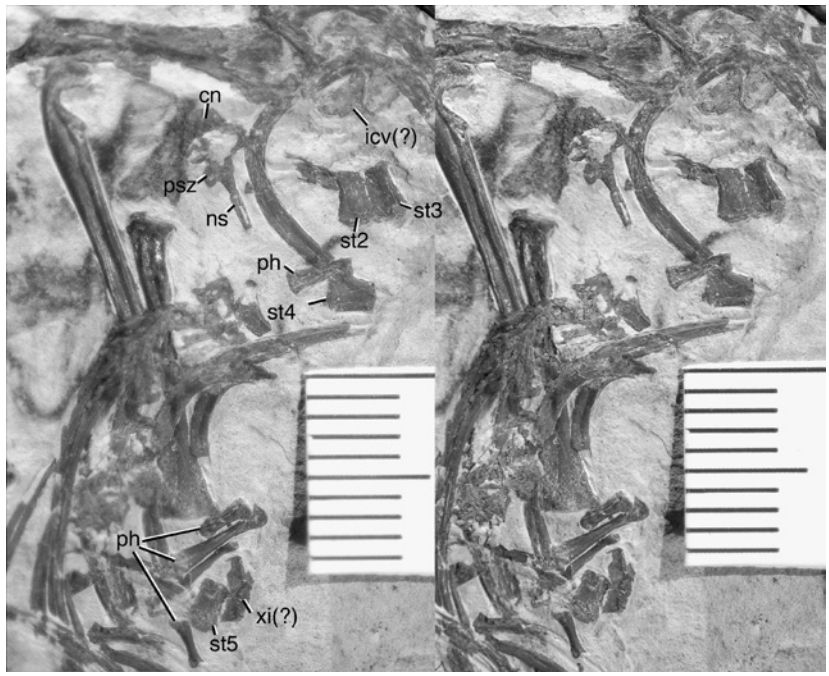

Fig. 3. Axial skeletal elements preserved in *Zhangheotherium* (CAGS97-07352). (A) Stereo photos of the sternal and some thoracic elements (CAGS97-07352). Abbreviations: cn, centrum; icv(?), questionable interclavicle; psz, postzygapophysis; ns, neural spine; ph, phalanges; st1-st4, sternebrae 1 through 4; xi(?) questionable xiphoid process of sternal series. Arrows points to a mid-thoracic vertebra (with posterior inclined neural spine).

articulating relationship of this element to the clavicle is unknown because the latter is not preserved in this specimen, so the identification of the interclavicle remains tentative. The four identifiable sternal elements of this juvenile are not fused together as is the case of the subadult type specimen of *Zhangheotherium*. The unsegmented sternum may be due to fusion in the due course of skeletal ontogeny in an older individual.

One isolated thoracic vertebra from the anterior thorax shows a posteriorly inclined neural spine. The spine is tall and twice the height of the vertebral centrum. Five lumbar vertebrae are present. Although heavily damaged, all lumbar vertebrae have preserved traces or outlines of the anteriorly inclined neural spines, with the spine being the tallest in lumbar 5 (posterior), but becoming successively shorter in the more anterior lumbar vertebrae. None of the lumbar vertebrae in CAGS97-07352 and the holotype of *Zhangheotherium* have the large and anteriorly slanted transverse process of the lumbar vertebrae as in multituberculates (Krause and Jenkins, 1983; Kielan-Jaworowska and Gambaryan, 1994). The ultimate thoracic vertebra (T13) has no neural spine, and most probably is the anticlinal vertebra (*sensu* Jenkins and Parrington, 1976). Hu *et al.* (1997) tentatively identified four sacral vertebrae in the holotype of *Zhangheotherium*, on the basis of the impression outlines. In CAGS97-07352, only three sacral vertebrae are present, as identified by their expanded transverse processes for the ilio-sacral contact. This count is similar to the intact pelvic and sacral area in *Maotherium* (NGMC 97415). So we determined that *Zhangheotherium* has three sacral vertebrae only.

Pelvis

The ilium is long and rod-like (Figs. 4 and 5). Its anterior part is plate-like in both known specimens of *Zhangheotherium*. The anterior ends of the ilia are strongly reflected laterally in ventral view (as preserved in IVPP 7466). The portion of the ilium between the ilio-sacral joint and the acetabulum is triangular in cross section; anteriorly the ilium has a prominent lateral iliac crest that divides a narrow dorsal surface and a broad concave ventro-lateral surface (Fig. 5). All these are typical of the mammalian ilium.

The ischium has a broad and flat posterior plate but its acetabular part is much thickened and forms a robust dorsal rim for the acetabulum (Figs. 4 and 5). The dorsal margin of the ischium is concave and curved posteriorly to a dorsally pointed ischial tuberosity. The posterior (and medial) margin of the ischium is uniformly convex and smooth, and it lacks any sign of postobturator notch (foramen) that is typical of multituberculates (Kielan-Jaworowska, 1979; Krause and Jenkins, 1983; Kielan-Jaworowska and Gambaryan, 1994).

An almost complete right pubis is exposed in lateral (ventral) view (Figs. 4–6). The preserved part bears the antero-ventral segment of the acetabular rim, and a part of the acetabular notch. The anterior border of pubis is curved; its medial part has a rugose area for articulating with the epipubis. A section of the pubic symphysis is also preserved (visible in Fig. 4; reconstructed in Fig. 5A). The epipubis is 7.7 mm in length, wider in its posterior portion than its anterior part. The posterodorsal border to contact the pubis is oriented obliquely from the main axis of the epipubis.

The acetabulum for articulating with the femoral head has a thickened dorsal rim and there is no cotyloid notch. The dorsal rim for the acetabulum is formed by the ilium and the ischium, as preserved in good condition in IVPP 7466. The pubic portion of the acetabulum rim is visible on the right pubis of CAGS97-07352 (Fig. 4). Inferring from the

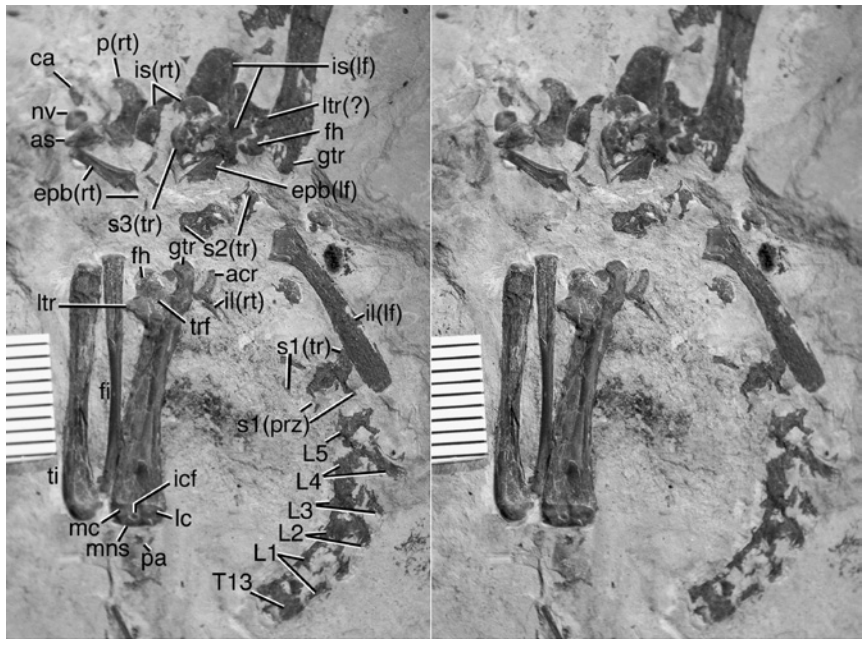

Fig. 4. Stereo photos of pelvis, lumbar, and sacral vertebrae and hindlimb of *Zhangheotherium* as preserved in CAGS97-07352. Abbreviations: acr, rim of acetabulum (partially preserved on right ilium and pubis); as, astragalus; ca, calcaneus; epb, epipubis; fh, femoral head; fi, fibula; gtr, greater trochanter of femur; icf, intercondylar fossa (of the femur); is, ischium; lc, lateral articular condyle of distal femur; (lf), left side; ltr, lesser trochanter of femur; L1, L2, L3, L4, L5, lumbar vertebrae 1 through 5; mc, medial articular condyle of distal femur; mns, fossilized meniscus cartilage of the knee joint; nv, navicular; p, pubis; pa, patella (partially ossified and fossilized); (rt), right side; s1(prz) and s1(tr), prezygapophysis and transverse process of sacral vertebra 1; s2, s3, sacral vertebrae 2 and 3; st2–st5, the second through the fifth sternebae; ti, tibia; trf, trochanteric fossa (on the femur); T13, the ultimate thoracic vertebra (the anticlinal vertebra).

acetabular sutures of the disarticulated ilium, ischium and pubis, each bone contributed to about one-third of the acetabulum. The obturator borders of the ischium and pubis, although not entirely complete, provides much of the outline for the obturator foramen. The obturator foramen is oval to oblong. Its medio-lateral dimension (width) is about the same as the acetabulum and its antero-posterior dimension (length) is longer than the diameter of the acetabulum. Its lesser diameter (width) is certainly larger than the narrowest possible width of pubis and than the breadth of the posterior plate of ischium. Relative to the rest of the pelvis, the obturator foramen of *Zhangheotherium* is larger than those in multituberculates and monotremes (Kielan-Jaworowska, 1975; Kielan-Jaworowska and Gambaryan, 1994), but smaller proportionately than the obturator foramina of *Henkelotherium*, *Vincelestes*, and the Cretaceous taxa of crown therians (Krebs, 1991; Rougier, 1993; Novacek *et al*., 1997; Ji *et al*., 2002; Luo *et al*., 2003).

Hindlimb

The femoral head is fully spherical, dorsomedially directed, and set-off by the femoral neck that graded into the shaft at roughly 60° (Figs. 4 and 5). The greater trochanter is

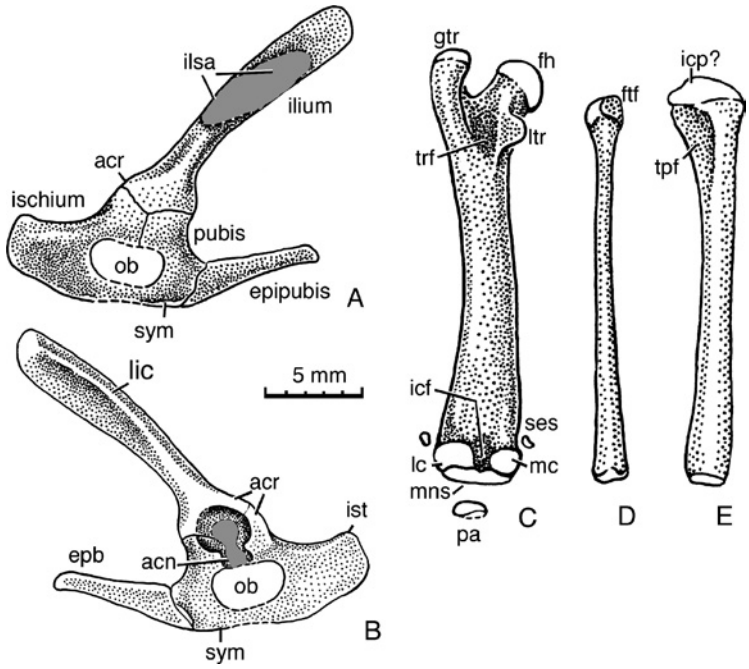

Fig. 5. Restoration of the pelvis and hindlimb of *Zhangheotherium*. (A) Restoration of pelvis (left, dorsomedial or internal view; based on CAGS97-07352; length of ilio-sacral contact is based on combined length of the preserved sacral transverse processes, but depth of this contact is uncertain). (B) Restoration of pelvis (left, ventrolateral or external view; composite restoration from CAGS97-07352 and a cast of IVPP 7466; gray pattern represents the damaged area of acetabulum). (C) Femur (left, posterior view, composite restoration of CAGS97-07352 and IVPP 7466). (D) Fibula (left, posterior view, composite restoration of two fibulae of CAGS97-07352). (E) Tibia (left, posterior view, composite restoration of two tibias of CAGS97-07352). Abbreviations: acr, rim of acetabulum (partially preserved on right ilium, ischium, and pubis); fh, femoral head; ftf, proximal fibulo-tibial facet (on fibula); gtr, greater trochanter of femur; icf, intercondylar fossa (of the femur); icp?, intercondyloid prominence?; ilsa, ilio-sacral joint area; ist, ischial tubercle; lc, lateral articular condyle of the distal femur; lic, lateral iliac crest; mc, medial articular condyle of the distal femur; ob, obturator foramen; ses, sesamoid bones above the distal femoral condyles; sym, pubic symphysis; tpf, tibialis posterior fossa (on tibia); trf, trochanteric fossa (of femur). Gray areas represent incomplete or damaged areas in the iliosacral joint and in the acetabulum notch, yet to be confirmed from future and better specimens; dash-lines are restoration based on incomplete outlines.

robust, and extends vertically from the shaft and beyond the femoral head, with a slightly expanded and in-turned apex that was the insertion of the gluteal muscles. The lesser trochanter is attached to the posterior aspect of the neck and has a triangular outline. The orientation of the lesser trochanter is such that it is projected posteriorly, and would be almost hidden from the anterior view of an intact femur. This is clear from the fact that the outline of the femur in IVPP 7466 failed to show the lesser trochanter in anterior view. The trochanteric fossa is represented by a nearly triangular depression between the greater and the lesser trochanters (Fig. 5). The shaft is relatively small in diameter below

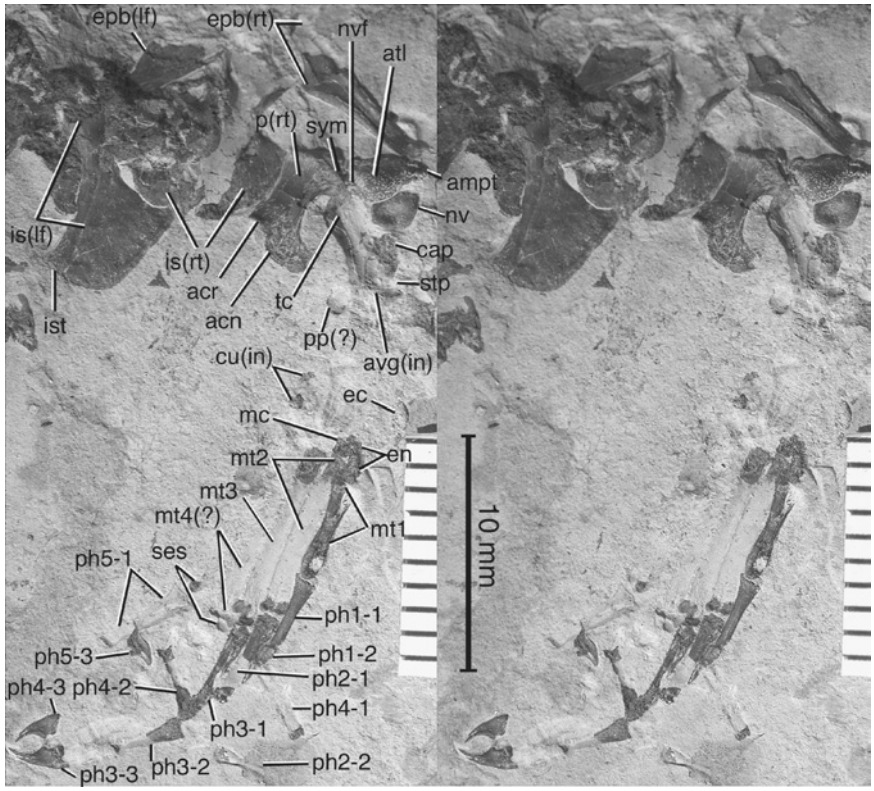

Fig. 6. Stereo photos of tarsal and pedal features of *Zhangheotherium*. (A) Preserved tarsal and pedal elements of CAGS97-07352. Abbreviations: acr, rim of acetabulum (on pubis); acn, acetabular notch (damaged; on pubis); ampt, astragalar medial proximal tubercle (on astragalus); atl, lateral astragalo-tibial facet (on astragalus); avg(in), anteroventral groove (on ventral aspect of calcaneus; incomplete and damaged); cap, calcaneo-fibular process (on calcaneus); cu(in), cuboid (incomplete and fragmented); ec, ectocuneiform; en, entocuneiform; epb(lf), epipubis-left (partial exposed); epb(rt), epipubis-right; mc, mesocuneiform; is(lf), ischium-left (complete, exposed in dorsomedial view); is(rt); ischium-right (broken and fragmented); ist, ischial tuberosity; mt1, mt2, mt3, mt4, and mt5, metatarsals 1, 2, 3, 4, and 5 (mt4 incomplete, mt5 lost); nv, navicular bone (exposed only in proximal view); ph, phalanx; ph1-1, -2, proximal and distal (claw) phalanges of pedal digit 1; ph2-1, -2, proximal and intermediate phalanges of digit 2 (distal phalanx is lost); ph3-1, -2, -3, proximal, intermediate and distal phalanges of digit 3; ph4-1, -2, -3, proximal, intermediate, and distal phalanges of pedal digital 4; ph5-1, -3; proximal and distal phalanges of digit 5 (intermediate phalanx is lost); pp(?), peroneal process (broken off from calcaneal body); p(rt), pubis-right (exposed in ventrolateral view); ses, paired sesemoid bones for digital flexors; stp; sustentacular facet and process (on calcaneus); sym, symphysis (on pubis); tc, calcaneal tuber (tuber calcis).

the level of the lesser trochanter, and becomes thicker distally. The distal end of the femur bears a clear epiphyseal suture between the shaft and the distal epiphysis. The two distal articulating condyles are formed by the epiphysis, and are separated by an intercondylar fossa in the posterior aspect of the femur. The lateral articular condyle is broader than the medial articular condyle (Figs. 4 and 5).

The proximal end of the tibia is capped by a dome-shaped epiphysis, with a distinctive suture to the diaphysis (shaft) (Fig. 5). The shape of the epiphysis is slightly asymmetrical,

and we interpret that the elevated portion of the epiphysis is a part of the inter-condyloid prominence as in extant therian mammals. The proximal epiphysis is expanded posteriorly and overhangs the posterior surface of the shaft. On the medio-posterior aspect of the tibia, there is a pronounced concave area, which is interpreted to be the fossa for the origination of M. tibialis posterior. The proximal half of the tibial shaft is asymmetrical and slightly bowed laterally. However, the tibia lacks the pronounced, hook-like dorsolateral process seen in multituberculates and monotremes. In this regard, *Zhangheotherium* is similar to extant therians (Szalay, 1994; Ji *et al*., 2002; Luo *et al*., 2003). There is no distinctive anterior tibial tuberosity and crest. The distal end of the tibia is flat and bears no medial maleolus.

The proximal end of the fibula is slightly expanded with an oblong outline in lateral view. The distal end of the fibula is truncated and has no styloid process. The fibula is narrower than the tibia, its diameter being about half the size of tibia near the middle part of the shaft. The fibula is slightly shorter than the tibia in the relatively well-preserved left hindlimb of CAGS97-07352 and the left hindlimb of IVPP 7466. From this we infer that the fibula did not directly contact the femur.

The patella is present, but incomplete as preserved on either hindlimb. A broken patella is visible near the distal end of the right femur; and a fragment of patella is preserved in association with the proximal end of the left fibula (Fig. 4). A fossilized (although incomplete) meniscus cartilage is attached to the distal articular condyles of the right femur. Two small sesamoid bones are preserved above the distal condyles of the femur. The medial sesamoid is likely to be for the gastrocnemius muscle and the lateral sesamoid for the popliteal muscle (Evans, 1995).

Tarsals

The calcaneal body is dorsoventrally depressed anteriorly and slightly compressed mediolaterally in the posterior part (Figs. 6 and 7). The calcaneo-cuboid facet (cuboid facet) is nearly flat, oriented transversely and positioned at the anterior end of the calcaneal body. The posterior end of the calcaneal tuber is expanded, slightly reflected medially. The ventral surface in the anterior part of the calcaneal body is flat to slightly concave. This is similar to the antero-ventral groove present in *Vincelestes* (Rougier, 1993), and in such Cretaceous eutherians as *Eomaia*, *Asioryctes*, and *Ukhaatherium* (Kielan-Jaworowska, 1977; Horovitz, 2000; Luo *et al*., 2003). There is no anteroventral tubercle that is characteristic of the calcanei in Cretaceous and Early Tertiary metatherians (Szalay, 1994; de Muizon, 1998; Luo *et al*., 2003). The peroneal process is projected laterally from the calcaneal body and the base of the peroneal process is offset from the cuboid facet by a shallow notch, which is for the peroneal ligament. In the medial aspect of the calcaneal body, the anterior (distal) facet for the astragalus (sustentacular facet) faces medially and its plane of contact with the astragalus is oriented vertically. The sustentacular facet is located on a slight protuberance from the calcaneal body in ventral view (Fig. 6: stp).

The contact structure of the calcaneo-astragalo-fibula is located mid-length of the calcaneus and posterior to the sustentacular facet, and it is on the medial side of the main axis of the calcaneus. In ventral view, this structure forms a slight protuberance (Fig. 6: cap). Located on this protuberance, the calcaneo-astragalar facet is faced medially and oriented vertically (Fig. 7F, G: caa). The posterior (proximal) process for the contact

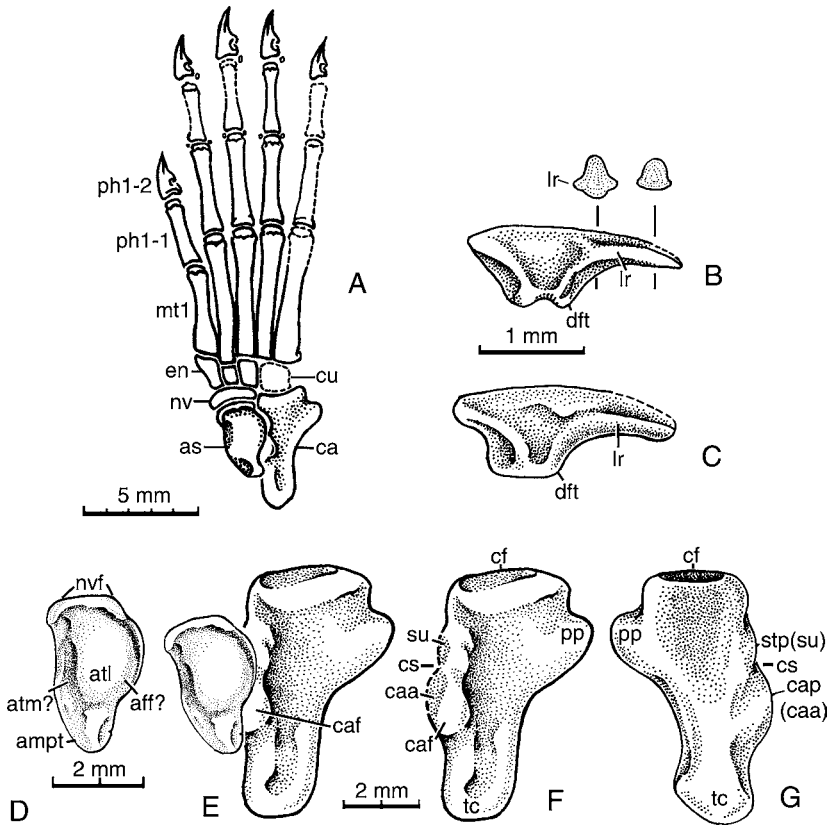

Fig. 7. Restoration of tarsal and pedal structure of *Zhangheotherium*. (A) composite restoration of pes (from CAGS97-07352 and the cast of IVPP 7466). (B) Pedal claw in lateral view and cross-section profiles. (C) Manual claw in lateral view. (D) Dorsomedial (proximal) view of astragalus (camera lucida drawing from CAGS97-07352). (E) topographic relationship of astragalus (in dorsal view, obliquely oriented to calcaneus) and calcaneus (in dorsal view). (F) calcaneus (dorsal view, without astragalus). (G) calcaneus (ventral or planter view). Abbreviations: as, astragalus; ampt, astragalar medial proximal tubercle; atm, medial astragalo-tibial facet (on astragalus); aff, astragalo-fibular facet (on astragalus); atl, lateral astragalo-tibial facet; ca, calcaneus; caa, calcaneo-astragalar contact (on medial side of calcaneus); caf, calcaneo-fibular facet (on calcaneus); cap(caa), calcaneo-astragalar process (bearing the sustentacular facet on its medial side); cf, calcaneo-cuboid facet (on calcaneus); dft, digital flexor tubercle; en, ento-cuneiform; lr, lateral ridge on distal phalanx (claw); mt, metatarsal; nv, navicular; nvf, navicular facet ("head" of astragalus); ph, phalanges; pp, peroneal process; stp(su), sustentacular facet and process; su, sustentacular facet (on medial side of the calcaneus).

between astragalus and the fibula is elevated from the calcaneal body (Fig. 7E, F: caf). This is a prominent structure visible on the dorsal aspect of the calcaneus, near its mid-length and medial to the longitudinal axis. This process bears two contact surfaces. The contact surface for the astragalus is faced medially. The calcaneo-fibular facet is facing dorsally. It appears from the morphology and size of the calcaneus and the astragalus that a significant part of the calcaneo-astragalo-fibular process is exposed dorsally whereas the astragalus is in juxtaposition with the calcaneus in the intact ankle. Therefore, a substantial

part of the calcaneo-astragalo-fibular process has contacted the distal end of the fibula. The slightly concave area between the sustentacular facet and the calcaneo-astragalar facet is tentatively identified as the calcaneal sulcus (Fig. 7: cs). The calcaneal structure described above is based on the restoration from camera lucida drawings of outlines and reversed stereo pair photographs and molds of the two calcanei in two specimens (cast of IVPP 7466; CAGS97-07352). It needs to be reconfirmed when the intact calcaneus of *Zhangheotherium* is discovered in the future.

The well-preserved astragalus is exposed in dorsal view (Figs. 6 and 7). The dorsal aspect of the astragalus is characterized by a broad convex structure, most of which is the facet for the tibia (Fig. 7: atl). The lateral margin of this convex structure may have contacted the distal end of the fibula. However, there is no distinctive crest to separate the tibial and the fibular facets. The anterior (distal) end of the astragalus is slightly expanded around the rim to form a largely flat navicular facet. The navicular facet is not separated by any distinctive neck from the tibial and fibular facets. This is similar to the astragalus of *Vincelestes* (Rougier, 1993) but different from the astragali of metatherians and eutherians (Kielan-Jaworowska, 1977; Szalay, 1994; Horovitz, 2000; Luo *et al*., 2003). Also the navicular facet is restricted anteriorly and is not spread medially as in metatherians (Szalay, 1994; Luo *et al*., 2003). In the posteromedial corner of the astragalus, there is a small but discernible astragalar medial planter tubercle. On the posterior part of the astragalus, the astragalar foramen is lacking. The ventral aspect of the astragalus is not exposed in CAGS97-07352.

Because of the orientation of the sustentacular facet on the calcaneus and the angle between the sustentacular facet and the calcaneo-astragalus facet, it is beyond any doubt that there is not much overlap of the astragalus over the calcaneal body. The medially facing astragalar facet and sustentacular facet, as preserved in *Zhangheotherium* (IVPP 7466; CAGS97-07352), are usually associated with "side-by-side" juxtaposition of the astragalus and the calcaneus in other mammals (Jenkins, 1970; Kielan-Jaworowska and Gambaryan, 1994; Szalay 1994; Ji *et al*., 1999). A full superposition of astragalus over the calcaneus is absent in *Zhangheotherium* (Fig. 7).

The navicular is a medio-laterally wide but proximal-distally short bone, with a concave proximal surface. We interpret the convex outline to be the dorsal side and the concave outline to be ventral (Figs. 6 and 7: nv). The cuboid is poorly preserved although discernible. It is represented by a depression (mold) in the shale with an oblong outline but has only two pieces of original bones within this depression. So the precise shape of the cuboid is unknown. The entocuneiform, identified by its articulation with metatarsal I, is twice as long as the mesocuneiform. The ectocuneiform has an oblong outline, with 75% the length of the entocuneiform. The mesocuneiform is the shortest and smallest of the three cuneiform bones. The proximal end of metatarsal II (corresponding to the mesocuneiform) is longer than metatarsals I and III, so the contact of the mesocuneiform with metatarsal II is offset from the metatarsal I and metatarsal III joints to the entocuneiform and the ectocuneiform, respectively. Paired sesamoid bones for the deep digital flexor muscle tendons are present in some joints between the metatarsals and proximal phalanges and at the interphalangeal joints. There is only a single, slightly larger sesamoid at the base of the distal phalanx 3–3 (the "claw"), same as in the eutherian *Eomaia* (Ji *et al*., 2002; Luo *et al*., 2003). On the basis of the preserved pedal elements of CAGS97-07352 and IVPP 7466, a composite restoration of the hind-foot is presented in Fig. 7.

DISCUSSION

The new specimen (CAGS97-07352) of *Zhangheotherium* has provided useful anatomical information, above and beyond what is already known for the skeletal anatomy and dental morphology for zhangheotheriids (Hu *et al*., 1997, 1998; Rougier *et al*., 1998). On the basis of this new fossil, we offer the following new comparative observations on its dental replacement pattern and tarsal characteristics.

As described above, *Zhangheotherium* has typical diphyodont dentition. Its premolars are replaced in alternating positions (p1 → p3 → p2) but in an antero-posterior direction (Fig. 2). We suggest here that this is the basal condition for the trechnotherian clade (herein defined by the common ancestor of [zhangheotheriids and spalacotheriids] + [marsupials + placentals]). The presence of the similar pattern of premolar replacement has been documented in several successive ranks of taxa within the trechnotherian clade (Martin, 1997; Kobayashi *et al*., 2002; Luo *et al*., 2004).

An alternating and antero-posterior sequential replacement of all antemolars (including premolars) has been thoroughly documented in *Dryolestes* with extensive data (Martin 1997, 1999). In *Dryolestes*, the premolar replacement (both shedding of deciduous teeth and eruption of permanent teeth) is characterized as: p1 → p3 → p2 → p4. The diphyodont replacement, at least in the lower jaw, occurs in the antero-posterior direction by two waves. The first replacing wave consists of i2, i4, p1, p3, which are followed by the second wave of i1, i3, c, p2, and p4. p4 is the last premolar to erupt, just prior to eruption of the sixth molar (m6) (Martin, 1997). In the boreosphenidan clade, a more restricted sub-clade within the trechnotherians, the premolar replacement also has an alternating pattern. The replacement sequence of premolars in the stem boreosphenidan "*Slaughteria*" is characterized by: p3 → p2 → p4 (Kobayashi *et al*., 2002). It is clear from this evidence that the alternating premolar replacement (p3 → p2 → p4) is consistently present from spalacotheriids through dryolestids to stem northern tribosphenic mammals in three different hierarchies of therian mammal phylogeny, suggesting that this is a widespread condition for all basal trechnotherian lineages (including the basal eutherians) (Luo *et al*., 2004).

The alternating premolar replacement in trechnotherians differs from the alternating dental replacements in premammalian cynodonts in having much reduced replacement rates, and in being limited to only one generation of successor per tooth locus, and only for antemolars. The replacement occurs in the antero-posterior direction. By contrast, the alternating replacement in many premammalian cynodonts has a faster rate, with multiple generations of successors; the replacement occurs in all tooth position, including the posterior postcanines. In those cynodonts with the alternating and frequent replacement, the replacement proceeds in the postero-anterior direction.

The trechnotherian premolar replacement is also different from the basic dental replacement pattern in the majority of mammaliaforms and stem mammals for which the dental replacement pattern is known. In *Sinoconodon*, replacements of the incisors and canine occurred multiple times in alternating waves for the duration of the individual life; but the premolariforms are replaced sequentially (rather than alternately) (Zhang *et al*., 1998; Luo *et al*., 2004). In other major basal mammalian groups, such as *Haldanodon*, *Morganucodon*, most multituberculates, *Gobiconodon*, and triconodontids, all premolars (or deciduous molariforms) are being replaced in antero-posterior sequence (Jenkins and Schaff, 1988; Greenwald, 1988; Martin and Nowotney, 2000; Nowotny *et al*., 2001; Wang *et al*., 2001; Luo *et al*., 2004; Kielan-Jaworowska *et al*., 2004). Therefore, the alternating

replacement (at least for p3 → p2 → p4) in trechnotherians is different from the primitive pattern of the antero-posterior sequential replacement of postcanines in all mammal groups outside the trechnotherian clade. This alternating replacement is an apomorphy of the trechnotherians.

Tarsal Features

The ankle joint of *Zhangheotherium* has a mosaic of primitive and derived characters. In the following discussion we will divide these features in three categories related to the ranks of phylogenetic hierarchies: (1) plesiomorphies of mammaliaforms; (2) plesiomorphies shared by multituberculates and trechnotherians; and (3) apomorphies of trechnotherians.

Mammaliaform Plesiomorphies

The side-by-side juxtaposition of the astragalus and the calcaneus, as evidenced in currently available specimens of *Zhangheotherium*, is a primitive feature of *Morganucodon* and eutriconodontans. Some of these features are even present in tritylodontid cynodonts. However, the astragalus–calcaneus juxtaposition is a variable feature in multituberculates. In the most primitive known multituberculate with preserved ankle joint (*Sinobaatar*), the astragalus and the calcaneus are in juxtaposition, as preserved. The superposition of these two bones is not developed (Hu and Wang, 2002). In the Late Cretaceous djadochtatherian multituberculates from Mongolia, the astragalus is oriented obliquely relative to the calcaneal body, and does not overlap the calcaneus, according to the detailed restoration by Kielan-Jaworowska and Gambaryan (1994). Coupled with the relatively new information from *Sinobaatar*, this is clearly the diagnostic condition for the multituberculates as a group. Nonetheless, within multituberculates, *Ptilodus* and *Eucosmodon* have developed a partial superposition of the astragalus and the calcaneus (Krause and Jenkins, 1983). The superposition of the astragalus and calcaneus is no better developed in *Zhangheotherium* than in the Late Cretaceous multituberculate *Kryptobaatar*.

Related to the primitive juxtaposition of the astragalus and calcaneus are: medial placement and vertical orientation of the sustentacular and the posterior calcaneo-astragalar facets. Both these features contributed to the side-by-side arrangement of the astragalus and the calcaneus, and are primitive. The calcaneo-astragalo-fibular process is in contact with the distal end of the fibula; therefore there is a relatively large facet of the calcaneus and the distal fibula; these are primitive features of monotremes, eutriconodontans and some multituberculates.

Theriiform Plesiomorphies

The group of multituberculates and trechnotherians (Theriiformes, *sensu* Rowe, 1988) can be characterized by several characters in the astragalus and calcaneus. These include: presence of a distinctive peroneal process (instead of a broad shelf) and a prominent peroneal notch between the cuboid facet and the peroneal process. The relatively compressed calcaneal tuber. These two features have been invoked to support the relationship of multituberculates and trechnotherians (Rowe, 1988; for a review of this complex issue, see Luo *et al*., 2002: p. 32–33). The calcaneus of *Zhangheotherium* also resembles those of multituberculates in a narrower anterior portion of the calcaneal body, in comparison to

eutriconodontans and *Morganucodon* (Jenkins and Parrington, 1976; Szalay, 1994; Ji *et al*., 1999).

Trechnotherian Apomorphies

The astragalus of *Zhangheotherium* has two apomorphies that are not present in multituberculates, eutriconodontans, and morganucodontans. The periphery of the navicular facet on the astragalus has an expanded rim, so that the astragalo-navicular contact appears to be much more prominent. This feature is not present in multituberculates, the eutriconodontan *Jeholodens* and *Morganucodon* (Jenkins and Parrington, 1976; Krause and Jenkins, 1983; Kielan-Jaworowska and Gambaryan, 1994; Ji *et al*., 1999). In the postero-medial area of the astragalus, there is a small but distinctive astragalar medial planter tubercle ("ampt" of Horovitz, 2000; Luo *et al*., 2003). This structure is absent or poorly developed in multituberculates, eutriconodontans, and *Morganucodon* (Krause and Jenkins, 1983; Kielan-Jaworowska and Gambaryan, 1994; Szalay, 1994; Ji *et al*., 1999). The astragalar medial planter tubercle is better developed and has the shape of a crest in the Cretaceous eutherians *Ukhaatherium* (Horovitz, 2000) and *Eomaia* (Luo *et al*., 2003), although this structure is more reduced in the Cretaceous metatherians (Szalay, 1994; Luo *et al*., 2003). We suggest that the expanded rim of the astragalo-navicular facet and the development of the astragalar medial proximal tubercle are apomorphies of the trechnotherian clade (zhangheotheriids + metatherians + eutherians), as can be corroborated by the congruence of other apomorphies for the trechnotherian clade (McKenna, 1975; Prothero, 1981; Luo *et al*., 2002). At the anterior end of the calcaneal body, the calcaneo-cuboid facet is transversely oriented, similar to the condition in *Vincelestes* (Rougier, 1993) and Cretaceous eutherians (Horovitz, 2000; Luo *et al*., 2003). This can also be an apomorphy of the trechnotherian clade. Therefore, the new fossil of *Zhangheotherium* has shown some apomorphic tarsal characters that can be used to diagnose the trechnotherian clade.

Absence of superposition of the calcaneus and the astragalus in *Zhangheotherium* indicates that the trechnotherian clade as a whole has retained the primitive condition of mammaliaforms in this key feature of the ankle joint. Recent and new evidence shows that the astragalus and the calcaneus have not achieved complete super-positional relationship in the earliest metatherians (*Sinodelphys*) and eutherians (*Ukhaatherium* and *Eomaia*). Although numerous metatherians and eutherians in the Tertiary have complete super-position of these two bones, the latest discoveries of *Sinodelphys*, *Eomaia*, and *Ukhaatherium*, as well as *Zhangheotherium* suggest that the superposition of astragalus and calcaneus were not achieved in the earliest-known members of the metatherian and eutherian lineages, neither in their proximal relatives. This derived feature evolved in parallel in metatherians and eutherians.

ACKNOWLEDGMENTS

This study is offered as a tribute to Professor William A. Clemens, Jr, in recognition of his classic studies of the Cretaceous mammals of North America and his many other important contributions to our understanding of early mammalian evolution. For more than four decades, Bill has been a mentor for many students at the University of Kansas and the University of California at Berkeley, including the first author of this paper. Zhe-Xi Luo is deeply indebted to Bill for his tutelage and training during his graduate studies. We are

delighted that this study can be a part of the Festschrift volume in honor of Bill Clemens. During the course of this work, we benefited from discussion with our colleagues K. C. Beard, M. R. Dawson, W. P. Luckett, T. Martin, and J. R. Wible. We also benefited from having a cast of IVPP 7466, made available by Prof. C.-K. Li and Y.-Q. Wang and Mr. Y.-M. Hu. We thank M. R. Dawson, Thomas Martin and P. David Polly for their useful comments and editorial help. M. A. Klingler assisted with graphics. This research was supported by the National Geographic Society (Q. Ji and Z.-X. Luo), the National Science Foundation of USA (DEB-95278902, DEB 0316558 to Zhe-Xi Luo), National Science Foundation of China (NSFC40328004 to Zhe-Xi Luo), Ministry of Land Resources, and Ministry of Science and Technology of People's Republic of China (Q. Ji), and the Carnegie Museum of Natural History (Z.-X. Luo).

LITERATURE CITED

Averianov, A. O. (2002). Early Cretaceous "symmetrodont" mammal *Gobiotheriodon* from Mongolia and the classification of "Symmetrodonta." *Acta Palaeontol. Polon.* **47:** 705–716.

Cifelli, R. L. (1999). Therian teeth of unusual design from the medial Cretaceous (Albian–Cenomanian) Cedar Mountain Formation, Utah. *J. Mammal. Evol.* **6:** 247–270.

Cifelli, R. L., and Madsen, S. K. (1999). Spalacotheriid symmetrodonts (Mammalia) from the medial Cretaceous (upper Albian or lower Cenomanian) Mussentuchit local fauna, Cedar Mountain Formation, Utah, USA. *Geodiversitas* **21:** 167–214.

Crompton, A. W. (1971). The origin of the tribosphenic molar. In: *Early Mammals*, D. M. Kermack and K. A. Kermack, eds., pp. 65–87, *Zool. J. Linn. Soc.* 50, London.

Crompton, A. W., and Jenkins, F. A., Jr. (1967). American Jurassic symmetrodonts and Rhaetic "pantotheres." *Science* **155:** 1006–1009.

Crompton, A. W., and Luo, Z.-X. (1993). Relationships of the Liassic mammals *Sinoconodon*, *Morganucodon*, and *Dinnetherium*. In: *Mammal Phylogeny: Mesozoic Differentiation, Multituberculates, Monotremes, Early Therians, and Marsupials*, F. S. Szalay, M. J. Novacek, and M. C. McKenna, eds., pp. 30–44. Springer-Verlag, New York.

Evans, H. E. (1995). *Miller's Anatomy of The Dog (*3rd edn.), Saunders, New York.

Fox, R. C. (1976). Addition to the mammalian local fauna from the upper Milk River Formation (Upper Cretaceous), Alberta. *Can. J. Earth Sci.* **13:** 1105–1118.

Fox, R. C. (1985). Upper molar structure in the Late Cretaceous symmetrodont *Symmetrodontoides* Fox, and a classfication of the Symmetrodonta (Mammalia). *J. Paleontol.* **59:** 21–26.

Gill, P. (2004). A new symmetrodont from the Early Cretaceous of England. *Journal of Vertebrate Paleontology* **24:** 748–752.

Greenwald, N. S. (1988). Patterns of tooth eruption and replacement in multituberculate mammals. *J. Vertebr. Paleontol.* **8:** 265–277.

Horovitz, I. (2000). The tarsus of *Ukhaatherium nessovi* (Eutheria, Mammalia) from the Late Cretaceous of Mongolia: an appraisal of the evolution of the ankle in basal therians. *J. Vertebr. Paleontol.* **20:** 547–560.

Hu, Y-M., and Wang, Y.-Q. (2002). *Sinobataar* gen. nov.: First multituberculate from Jehol Biota of Liaoning, Northern China. *Chin. Sci. Bull.* **47:** 933–938.

Hu, Y.-M., Wang, Y.-Q., Luo, Z.-X., and Li, C.-K. (1997). A new symmetrodont mammal from China and its implications for mammalian evolution. *Nature* **390:** 137–142.

Hu, Y.-M., Wang, Y.-Q., Li, C.-K., and Luo, Z.-X. (1998). Morphology of dentition and forelimb of *Zhangheotherium*. *Vertebrata PalAsiatica* **36:** 102–125.

Hu, Y.-M., Meng, J., Wang, Y.-Q., and Li, C.-K. (2005). Large Mesozoic mammals fed on young dinosaurs. *Nature*. **433:** 149–153.

Jenkins, F. A., Jr. (1970). Cynodont postcranial anatomy and the "prototherians" level of mammalian organization. *Evolution* **24:** 230–252.

Jenkins, F. A., Jr., and Parrington, F. R. (1976). The postcranial skeletons of the Triassic mammals *Eozostrodon*, *Megazostrodon* and *Erythrotherium*. *Philos. Trans. R. Soc. Lond.* **273:** 387–431.

Jenkins, F. A., Jr., and Schaff, C. R. (1988). The Early Cretaceous mammal *Gobiconodon* (Mammalia, Triconodonta) from the Cloverly Formation in Montana. *J. Vertebr. Paleontol.* **6:** 1–24.

Ji, Q., Luo, Z.-X., and Ji, S. (1999). A Chinese triconodont mammal and mosaic evolution of the mammalian skeleton. *Nature* **398:** 326–330.

Ji, Q., Luo, Z.-X., Yuan, C.-X., Wible, J. R., Zhang, J.-P., and Georgi, J. A. (2002). The earliest known eutherian mammal. *Nature* **416:** 816–822.

Kielan-Jaworowska, Z. (1975). Possible occurrence of marsupial bones in Cretaceous eutherian mammals. *Nature* **255:** 698–699.

Kielan-Jaworowska, Z. (1977). Evolution of the therian mammals in the Late Cretaceous of Asia. Part II. Postcranial skeleton in *Kennalestes* and *Asioryctes*. *Palaeontol. Polon.* **37:** 65–83.

Kielan-Jaworowska, Z. (1979). Pelvic structure and nature of reproduction in Multituberculata. *Nature* **277:** 402–403.

Kielan-Jaworowska, Z., and Dashzeveg, D. (1998). Early Cretaceous amphilestid ("triconodont") mammals from Mongolia. *Acta Palaeontol. Polon.* **43:** 413–438.

Kielan-Jaworowska, Z., and Gambaryan, P. P. (1994). Postcranial anatomy and habits of Asian multituberculate mammals. *Fossils Strata* **36:** 1–92.

Kielan-Jaworowska, Z., Cifelli, R. L., and Luo, Z.-X. (2004). *Mammals from the Age of Dinosaurs: Origins, Structure, and Evolution,* Columbia University Press, New York.

Kobayashi, Y., Winkler, D. A., and Jacobs, L. L. (2002). Origin of the tooth-replacement pattern in therian mammals: Evidence from a 110 Myr old fossil. *Proc. R. Soc. Lond.* **269:** 369–373.

Krause, D. W., and Jenkins, F. A. (1983). The postcranial skeleton of North American multituberculates. *Bull. Mus. Comp. Zool.* **150:** 199–246.

Krebs, B. (1991). Das Skelett von *Henkelotherium guimarotae* gen. et sp. nov. (Eupantotheria, Mammalia) aus dem Oberen Jura von Portugal. *Berliner geowissenschafliche Abhandlungen* A **133:** 1–110.

Li, J.-L., Wang, Y., Wang, Y.-Q., and Li, C.-K. (2001). A new family of primitive mammals from the Mesozoic of western Liaoning, China. *Chin. Sci. Bull.* **46:** 782–785.

Li, C.-K., Wang, Y.-Q., Hu, Y.-M., and Meng, J. (2003). A new species of *Gobiconodon* (Triconodonta, Mammalia) and its implications for the age of Jehol Biota. *Chin. Sci. Bull.* (English Edition) **48:** 1129–1134.

Lo, C.-H., Chen, P.-J., Tsou, T.-Y., Sun, S.-S., and Lee, C.-Y. (1999). $^{40}Ar/^{39}Ar$ laser single grain and K-Ar dating of Yixian Formation, NE China. In: *Jehol Biota*, P.-J. Chen and F. Jin, eds., pp. 328–340, Science Press, Beijing.

Luo, Z.-X., Ji, Q., and Ji, S. A. (2001). New evidence on dental replacement in symmetrodonts and its implications for mammalian evolution. *J. Morphol.* **248:** 256.

Luo, Z.-X., Kielan-Jaworowska, Z., and Cifelli, R. L. (2002). In quest for a phylogeny of Mesozoic mammals. *Acta Palaeontol. Polon.* **47:** 1–78.

Luo, Z.-X., Ji, Q., Wible, J. R., and Yuan, C.-X. (2003). An Early Cretaceous tribosphenic mammal and metatherian evolution. *Science* **302:** 1934–1940.

Luo, Z.-X., Kielan-Jaworowska, Z., and Cifelli, R. L. (2004). Evolution of dental replacement in mammals. In: *Fanfare for an Uncommon Paleontologist—Festschrift in Honor of Dr. Malcolm C. McKenna,* M. R. Dawson, and J. A. Lillegraven, eds., pp. 159–175. The Carnegie Museum of Natural History Bulletin **36**.

Martin, T. (1997). Tooth replacement in Late Jurassic Dryolestidae (Eupantotheria, Mammalia). *J. Mammal. Evol.* **4:** 1–18.

Martin, T. (1999). Dryolestidae (Dryolestoidea, Mammalia) aus dem Oberen Jura von Portugal. *Abhandlungen der Senckenbergischen Naturforschenden Gesellschaft* **550:** 1–119.

Martin, T., and Nowotny, M. (2000). The docodont *Haldanodon* from the Guimarota Mine. In: *Guimarota: A Jurassic Ecosystem*, T. Martin and B. Krebs, eds., pp. 91–96, Verlag Dr. Friedrich Pfeil, Munich.

McKenna, M. C. (1975). Toward a phylogenetic classification of the Mammalia. In: *Phylogeny of the Primates*, W. P. Luckett and F. S. Szalay, eds., pp. 21–46. Plenum, New York.

Mills, J. R. E. (1984). The molar dentition of a Welsh pantothere. *Zool. J. Linn. Soc.* **82:** 189–205.

de Muizon, C. (1998). *Mayulestes ferox*, a borhyaenoid (Metatheria, Mammalia) from the early Palaeocene of Bolivia. Phylogenetic and palaeobiologic implications. *Geodiversitas* **20:** 19–142.

Novacek, M. J., Rougier, G. W., Wible, J. R., McKenna, M. C., Dashzeveg, D., and Horovitz, I. (1997). Epipubic bones in eutherian mammals from the Late Cretaceous of Mongolia. *Nature* **389:** 483–486.

Nowotny, M., Martin, T., and Fischer, M. (2001). Dental anatomy and tooth replacement of *Haldanodon exspectatus* (Docodonta, Mammalia) from the Upper Jurassic of Portugal. *J. Morphol.* **248:** 268.

Prothero, D. R. (1981). New Jurassic mammals from Como Bluff, Wyoming, and the interrelationships of non-tribosphenic Theria. *Bull. Am. Mus. Nat. Hist.* **167:** 277–326.

Rougier, G. W. (1993). *Vincelestes neuquenianus* Bonaparte (Mammalia, Theria) un primitivo mamífero del Cretácico Inferior de la Cuenca Neuquina, Ph.D. Dissertation, Universidad Nacional de Buenos Aires, Buenos Aires.

Rougier, G. W., Wible, J. R., and Novacek, M. J. (1998). Implications of *Deltatheridium* specimens for early marsupial history. *Nature* **396:** 459–463.

Rougier, G. W., Ji, Q., and Novacek, M. J. (2003). A new symmetrodont mammal with fur impression from the Mesozoic of China. *Acta Geol. Sinica* **77:** 7–14.

Rowe, T. B. (1988). Definition, diagnosis, and origin of Mammalia. *J. Vertebr. Paleontol.* **8:** 241–264.

Sigogneau-Russell, D., and Ensom, P. C. (1998). *Thereuodon* (Theria, Symmetrodonta) from the Lower Cretaceous of North Africa and Europe, and a brief review of symmetrodonts. *Cretaceous Res.* **19:** 1–26.

Simpson, G. G. (1928). *A Catalogue of the Mesozoic Mammalia in the Geological Department of the British Museum*. Trustees of the British Museum, London.

Swisher, C. C., III, Wang, Y.-Q., Wang, X.-L., Xu, X., and Wang, Y. (1999). Cretaceous age for the feathered dinosaurs of Liaoning, China. *Nature* **398:** 58–61.

Szalay, F. S. (1994). *Evolutionary History of the Marsupials and an Analysis of Osteological Characters*, Cambridge University Press, Cambridge.

Wang, Y.-Q., Hu, Y.-M., Meng, J., and Li, C.-K. (2001). An ossified Meckel's cartilage in two Cretaceous mammals and origin of the mammalian middle ear. *Science* **294:** 357–361.

Zhang, F.-K., Crompton, A. W., Luo, Z.-X., and Schaff, C. R. (1998). Pattern of dental replacement of *Sinoconodon* and its implications for evolution of mammals. *Vertebr. PalAsiatica* **36:** 197–217.